Asymmetric zoning profiles in garnet from HP–HT granulite and implications for volume and grain-boundary diffusion

P. J. O'BRIEN

Bayerisches Geoinstitut, Universität Bayreuth, D-95440 Bayreuth, Germany

ABSTRACT

Detailed electron-microprobe line profiles and small-area compositional maps of zoned garnets in a sample of high-pressure–high-temperature granulite show features inconsistent with commonly applied diffusion models. Larger grains of an early garnet generation have their highest Ca contents in domains away from the rim or inclusions but show a sharp fall in Ca balanced by increased Mg and Fe (and slightly higher X_{Mg}) towards inclusions and the rim. In domains with secondary biotite, the sharp decrease in Ca is accompanied by variations in X_{Mg} dependent upon proximity to biotite, thus producing one-sided, asymmetric profiles with X_{Mg} lower against biotite. As a consequence, rim compositions of the same grain are different on the sides adjacent and away from biotite and there is no relationship between grain size and rim X_{Mg}. Such a zoning pattern requires that grain-boundary diffusion is as slow as volume diffusion and implies the absence of a diffusion-enhancing grain-boundary fluid phase during the majority of the rock's high-temperature exhumation history. Diffusion models ignoring this probability could yield either cooling rates that were too fast, or extrapolated ages based on closure temperature models that were too old.

A second garnet generation in the same rock, grown in a Ca-rich domain resulting from kyanite breakdown, has irregularly distributed patches, identified by compositional mapping, containing higher Ca than the first-formed garnet but at lower X_{Mg}. Use of such garnet compositions for geothermobarometrical determination of the high-pressure granulite stage would clearly lead to erroneous results. The presence of such contrasting garnet compositions in a granulite-facies rock is clearly evidence of disequilibrium, and further supports the proposition that there was a lack of an effective transport medium even at the mm scale.

KEYWORDS: garnet, zoning, diffusion, granulite.

Introduction

GEOTHERMOBAROMETRY in high-grade rocks of the granulite facies, even when retrogression has been avoided, is commonly hampered by the problems of diffusive resetting of mineral compositions along the cooling and exhumation path (e.g. Bégin and Pattison, 1994). Sometimes this lack of equilibrium can be used to our advantage. Compositional gradients within and between phases provide a record of the attempts of the respective phases to adapt to changing conditions. Diffusion modelling attempting to reproduce measured compositional gradients has been applied by numerous authors to quantify the timescales of pressure-temperature path segments (Lasaga *et al.*, 1977; Lasaga, 1983; Loomis *et al.*, 1985; Jiang and Lasaga, 1990; Chakraborty and Ganguly, 1990, 1992; O'Brien and Vrána, 1995, 1997; O'Brien, 1997; Brenker and Brey, 1997; Duchêne *et al.*, 1998). An evaluation of the modification of isotope concentrations and profiles by diffusive loss is also central to the determination of so-called 'closure temperatures' in geochronology (Dodson, 1973, 1986; Ehlers and Powell, 1994; Jenkin *et al.*, 1994). However, modelling of the observed diffusion-induced profiles requires not only a knowledge of interdiffusion coefficients in individual phases but also of transport rates and transport distances between exchanging phases. In

order to simplify the diffusion calculations it is commonly assumed in models that transport between phases along grain boundaries — grain-boundary diffusion — is orders of magnitude faster than volume diffusion within the phases (or at least one of the phases) of interest (Joesten, 1990). The assumption of fast grain-boundary diffusion is rarely questioned, but if this assumption is incorrect then such diffusion models are invalid. Here it will be shown how electron-microprobe line profiles and elemental mapping can be utilised to test the assumption of fast grain-boundary diffusion.

Geological setting

The largest granulite bodies in central Europe are concentrated in southern Bohemia, Czech Republic (Fiala et al., 1987; 1995), close to the town of Česke Budějovice (Fig. 1). The larger Blanský les (25 × 15 km), Křišt'anov, Prachatice and Lišov massifs (Fig. 1) are accompanied by much smaller bodies strewn along a NE–SW-trending belt for almost 100 km. The south Bohemian granulite bodies, like their counterparts in neighbouring Lower Austria, belong to the tectonically uppermost part of the Gföhl Unit. This unit is one of a series of nappe units that constitute the high-grade Moldanubian Zone of the southern Bohemian Massif (Fuchs, 1971, 1991, 1995; Fiala et al., 1995). The granulites enclose small bodies of serpentinised garnet peridotite, pyroxenites and sometimes also high-temperature eclogites (Medaris and Carswell, 1990; Medaris et al., 1995). The dominant granulites in south Bohemia, as elsewhere in the Variscides, are kyanite–K-feldspar-bearing (i.e. high-pressure-high-tempera-ture) varieties of granitic composition (e.g. Pin and Vielzeuf, 1983; Fiala et al., 1987); subordi-nate are clinopyroxene-bearing varieties and types with (probably) secondary orthopyroxene. A characteristic mylonitic fabric in the granulites, formed during exhumation accompanied by over-printing of the high-grade assemblage, generally hinders the recognition of the earlier history (Behr, 1978). All granulites in the Bohemian Massif were originally thought to be Precambrian in age (e.g. Neumann, 1984) but most geochronological studies, especially zircon and monazite dating, have yielded Palaeozoic, and in most cases Carboniferous, ages (van Breemen et al., 1982; Schenk and Todt, 1983; Aftalion et al., 1989; Quadt, 1993; Wendt et al., 1994; Kröner and Willner, 1995; Kotkova et al., 1996; O'Brien et

al., 1997a; Becker, 1997). Metamorphic condi-tions for the felsic granulites of the Bohemian Massif, deduced from less-overprinted domains of samples by determination of the original composi-tion of the now unmixed feldspars, are around 900−1050°C at pressures above 14 kbar (Carswell and O'Brien, 1993; O'Brien et al., 1997; Kryza et al., 1997; Kotková et al., 1996; Willner et al., 1997).

Sample description

All the following textural descriptions and mineral compositions come from a single hand specimen of felsic granulite from the quarry at Kobylí hora, 2 km NE of Prachatice in the Prachatice granulite complex (Fig. 1). The hand specimen of around 15 × 13 × 8 cm consists of the characteristically strongly foliated, light-coloured, Weiss-stein ('white-stone') granulite dotted with small (<0.5 mm) pink garnets either side of a 6 cm band containing significantly more abun-dant, and larger (dominantly 1 mm), garnets and dark biotite grains aligned parallel to the direction of the banding. The garnet-poor part is dominated by quartz and anti-perthitic feldspar enclosing small (generally 0.2−0.4 mm) garnets and minor trains of small (0.05−0.2 mm) grains of biotite defining the foliation. Accessory phases are apatite, zircon, rutile and ilmenite. Elongate quartz (up to 2 mm long) forms the largest grains whereas most of the feldspar either occurs in irregular-shaped subgrains or has recrystallised to a granoblastic two-feldspar (plagioclase X_{An} = 0.35−0.40 and K-feldspar) texture. Spinel (X_{Mg} = 0.36) is found in the core of plagioclase aggregates and as inclusions in garnet. In the garnet-rich zone, feldspar, quartz and garnet commonly contain elongate rutile needles. The quartz-feldspar texture is the same as in the garnet-poor part although larger (up to 2 mm) anti-perthite grains are often present for which a reconstituted composition of X_{An} = 0.207, X_{Ab} = 0.406, X_{Or} = 0.386 has been determined. Biotite (X_{Mg} = 0.60−0.64, TiO_2 ~5 wt.%) is more abundant in this zone and is commonly found at the edge of garnet, which it is clearly replacing (Fig. 2). The presence of spinel (and corundum) will be discussed in more detail later.

Textural and zoning characteristics of garnet

Garnet occurs in two texturally distinguishable generations. The texturally early garnet —
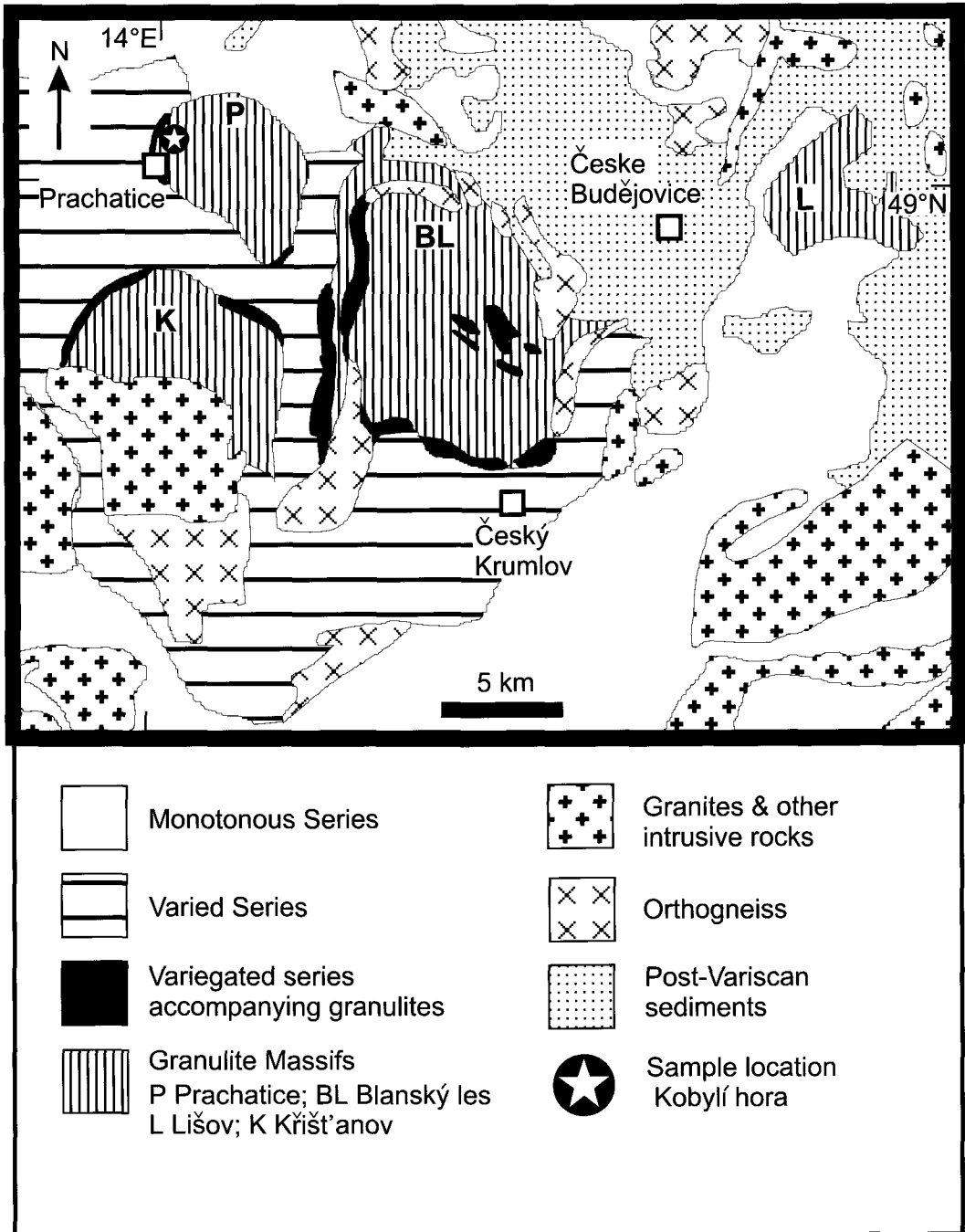
FIG. 1. Simplified geological map of Southern Bohemia showing granulite bodies and location of sample.

garnet1 — is larger, poikiloblastic to skeletal in form, and commonly encloses large inclusions of

anti-perthite and quartz along with apatite, zircon, rutile and rarely kyanite. It is generally in contact
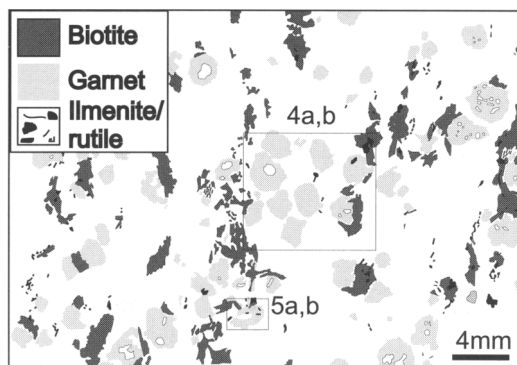
229

FIG. 2. Sketch of garnet and biotite distribution in a granulite thin section. Non-shaded areas represent feldspar, quartz and apatite. The locations for Figs 4 and 5 are marked.

with matrix anti-perthite grains. An additional characteristic of these garnets is the presence of anomalously elongate (mostly $100-300$ μm long and 1 μm wide) exsolved rutile needles in three orientations. The second generation garnet — garnet2 — forms chains, aggregates and coronas set within moats of plagioclase. However, anti-perthite grains are absent. This type of garnet commonly encloses spinel and/or ilmenite although plagioclase and corundum are also not uncommon as inclusions.

Compositional maps of garnet1 in parts of the sample without biotite, or with only scarce secondary biotite, typically show homogeneous interiors and strong zoning in Ca, Fe and Mg towards rims and around inclusion feldspars (Fig. 3). The zoning style is from a plateau with maximum X_{Ca} [X_{Ca} = Ca/(Ca+Mg+Fe+Mn)] around 0.12 and X_{Mg} [X_{Mg} = Mg/(Mg+Fe)] of around 0.37–0.38 to sharply zoned parts where X_{Ca} drops to 0.02 or less and both Fe and Mg rise such that X_{Mg} rises slightly (Fig. 3c). There is no substantial difference in the pattern of zoning between garnet and inclusion feldspar and garnet rims adjacent to matrix feldspars (Fig. 3c). In both cases, the Ca content of feldspar in contact with garnet is higher. The most important discovery in this sample was that X_{Mg} in garnet was strongly dependent upon its proximity to secondary biotite. This is illustrated by compositional maps in a domain containing several small grains of garnet1 flanked by parallel zones containing biotite (Fig. 4a,b). The compositional map (Fig. 4a) clearly shows that Mg decreases

significantly in the parts of garnet close to biotite. This is emphasised by decreasing X_{Mg} in garnet line profiles (Fig. 4c,f). The detailed line profiles also show that zoning may be non-concentric — i.e. one-sided — such that perpendicular line profiles across the same garnet are completely different parallel and perpendicular to the biotite foliation trend. This is nicely illustrated in Figs. 4e and f. In the profile parallel to the biotite foliation trend (Fig. 4e) a flat plateau-like interior composition with high Ca and X_{Mg} around 0.36 is zoned towards rims with much lower Ca and slightly higher X_{Mg} which is the typical garnet1 trend. In stark contrast, the perpendicular profile (Fig. 4f), although also showing falling Ca toward the rims, exhibits a very strong decrease in X_{Mg} towards the biotite-bearing domain such that the X_{Mg} trend is non-symmetric and rim X_{Mg} values are different on opposite sides of the same grain. It is clear in this domain that modification of garnet rim X_{Mg} is independent of garnet grain size but is directly dependent on proximity to biotite.

A compositional map of one of the small skeletal garnet2 grains (Fig. 5a) depicts one of the more interesting problems in this rock. In contrast to the plateau-like interior with respect to the Ca content of garnet1 (Fig. 3a), this map shows quite clearly that there are several small concentrations of Ca set randomly within garnet with a much lower average Ca content. There is no relationship, in the garnet as a whole, between proximity to garnet rim and Ca content. Instead one finds an irregular distribution of Ca-rich patches that may represent cores of early-grown parts of such chain-like garnets. A compositional profile across one of these Ca-rich domains (Fig. 5c) looks remarkably similar to that shown for a similar situation (i.e. garnet between inclusion and matrix feldspar) in garnet1 (Fig. 5d). However, important differences to note are the higher Ca content of garnet2 at a much lower X_{Mg} value. The Ca content is significantly higher even than the values obtained from the interior of garnet1 away from rims or inclusion feldspar and was probably even higher if the measured profile is considered as a frozen diffusion profile driven by the need for lower Ca at rims.

Pressure–temperature determination

Deducing $P-T$ conditions for the granulite-facies metamorphism in such a sample requires an assessment as to which garnet composition was
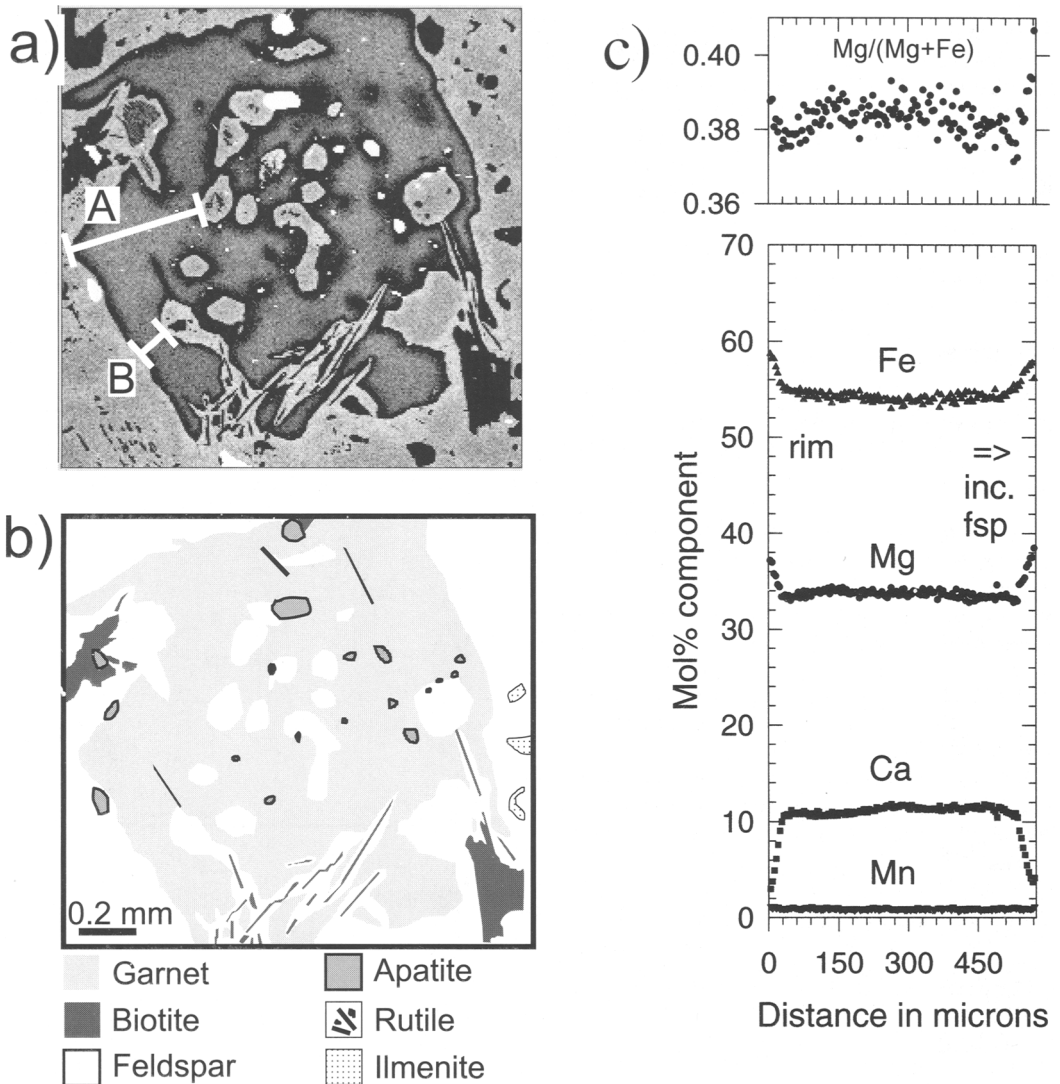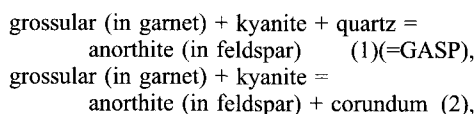
FIG. 3. (a) Garnet1 composition map (areas with low counts are dark, areas with higher counts are light) for the element Ca. 'A' marks the location of the profile in Fig. 3c, 'B' marks the location of the profile in Fig. 5d. (b) Textural sketch of the same area. (c) Typical zoning in garnet1 between rim and inclusion feldspar ('A' in Fig. 3a). The distance and Mg/(Mg+Fe) axes are equally scaled in this and all subsequent profiles.

in equilibrium with which matrix phases (and with which matrix-phase compositions) at a particular time. This is clearly no simple task in a situation where the main geobarometric information will be constrained by grossular component in garnet and anorthite component in feldspar. These are phases that both show significant compositional variation. The early
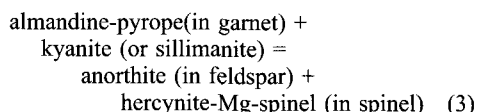
garnet in the sample, garnet1, probably formed in equilibrium with a melt in a paragenesis with ternary feldspar, quartz, kyanite and rutile (Vrána, 1989; Vrána and Jakeš, 1982; Carswell and O'Brien, 1993; Kotková and Harley, 1997). The high Ca content preserved in the interiors of garnet1 (Fig. 3c), combined with the reconstituted ternary feldspar, kyanite and quartz, yields

conditions of 1000°C, 18 kbar for the initial high-pressure granulite stage (Fuhrmann and Lindsley (1988) two-feldspar geothermometer, Koziol and Newton (1989) GASP geobarometry). The growth of biotite, most likely by a reaction such as Garnet + K-Feldspar + H$_2$O = Biotite + Plagioclase + Quartz, is clearly related to a modification in garnet X_{Mg}. Taking the range of biotite X_{Mg} from above (0.60–0.64 for matrix biotite not directly in contact with garnet), a zoned garnet such as in Fig. 4f and the garnet-biotite geothermometer of Ferry and Spear (1978), yields 750–850°C for pairings with garnet rim and values up to 150°C greater if the garnet core composition is utilised. Temperatures around 1000°C from garnet-biotite geothermometry would be consistent with the results from two-feldspar geothermometry. However, this is just fortuitous as the biotite-bearing stage is obviously later and garnet rims in parts away from biotite rise to higher X_{Mg} which would translate to even higher garnet-biotite temperatures! Considering just the minimum garnet-biotite temperature (i.e. deduced for garnet rim) implies that despite granulite-facies conditions, garnet compositions have not been reset and still preserve information relating to the early higher temperature stage.

Two distinct garnet domains or growth stages have been noted in granulites from elsewhere in the Bohemian Massif (Owen and Dostal, 1996; Willner et al., 1997) and the presence of corundum and/or spinel (and/or sapphirine) in Ca-rich domains surrounded by corona garnet (and the subsequent breakdown of the phases in these domains) has also been the subject of discussion (Carswell et al., 1989; Becker and Altherr, 1991; Carswell and O'Brien, 1993; Petrakakis and Jawecki, 1995; Owen and Dostal, 1996). In all these cases the spinel is a product of kyanite breakdown. This represents reactions such as:

grossular (in garnet) + kyanite + quartz =
anorthite (in feldspar)   (1)(=GASP),
grossular (in garnet) + kyanite =
anorthite (in feldspar) + corundum (2),

and

almandine-pyrope(in garnet) +
kyanite (or sillimanite) =
anorthite (in feldspar) +
hercynite-Mg-spinel (in spinel)   (3)

In such high-temperature rocks it is probable that these reactions are evidence for decompression trajectories (although heating following

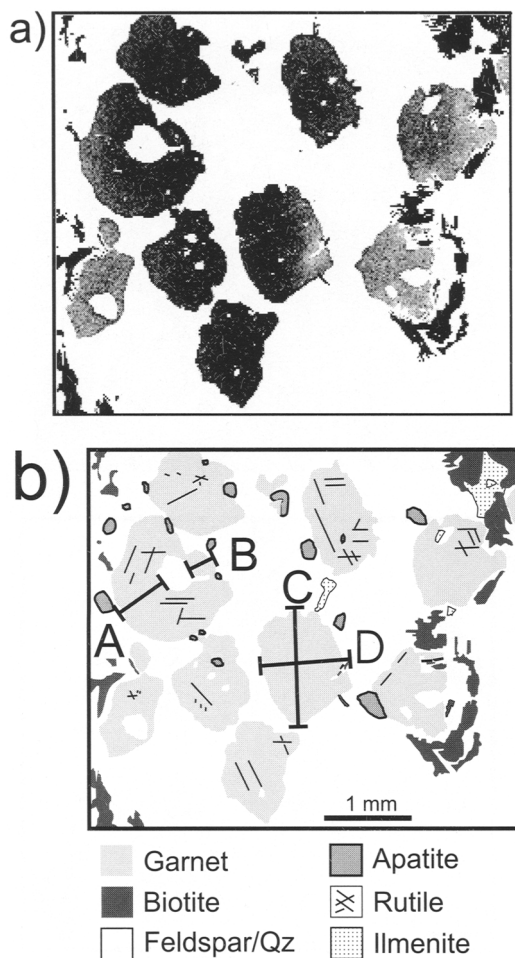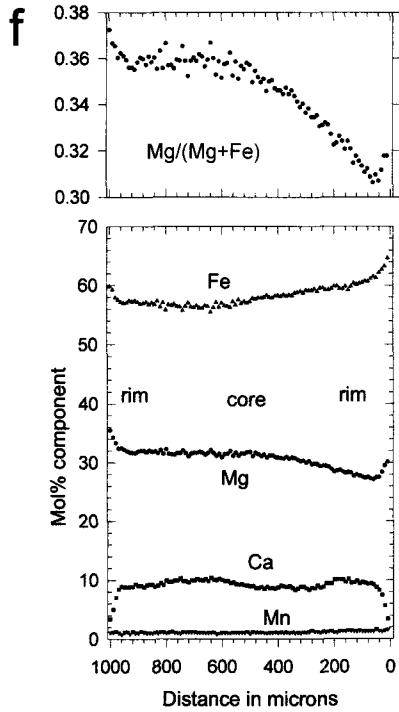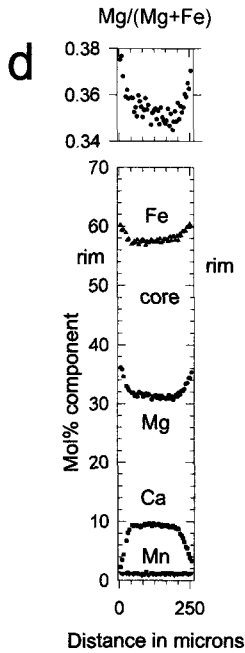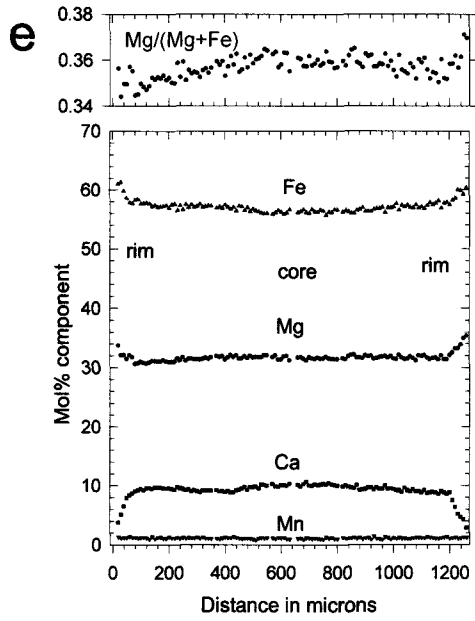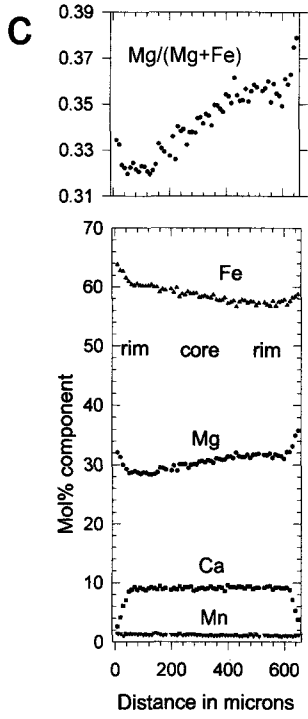FIG. 4. (a) Mg composition map (inverted scale so that light is low counts, dark is high counts) for a small domain with Garnet1 and secondary biotite. (b) Textural sketch of the same area. A, B, C, D, mark the locations of the profiles in Fig. 4c,d,e,f, respectively. (c) [opposite page] Profile 'A' in Fig. 4b, rim in biotite-bearing domain to inclusion feldspar. (d) Profile 'B' in Fig. 4b, between matrix and inclusion feldspar away from biotite zone. (e) Profile 'C' in Fig. 4b, parallel to biotite trend. (f) Profile 'D' in Fig. 4b, rim in biotite domain to rim away from biotite.

cooling cannot be ruled out completely). The reactions would explain the strong Ca-depletion in all garnet1 rims, the common Ca-rich nature of plagioclase in the spinel-bearing domains and the absence of kyanite in this particular sample (although kyanite rimmed by spinel-plagioclase
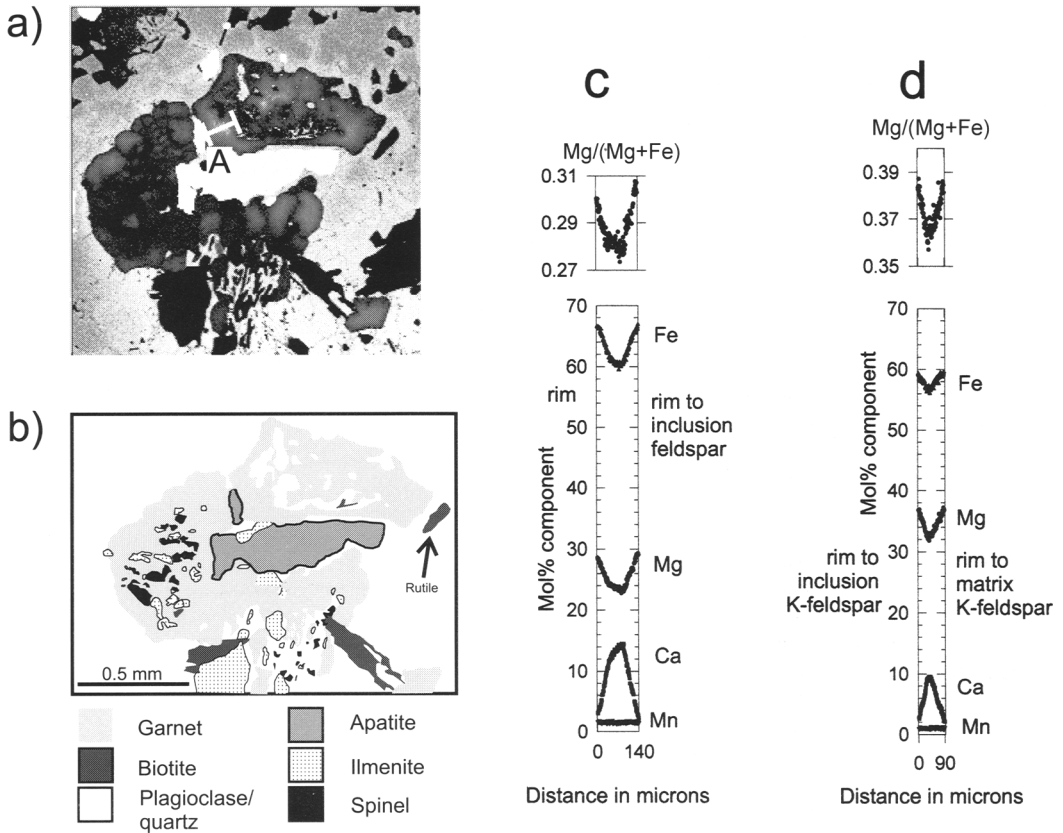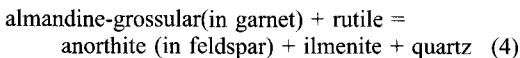
FIG. 5. (a) Garnet2 composition map (areas with low counts are dark, areas with higher counts are light) for the element Ca. 'A' marks the location of the profile in Fig. 5c. (b) Textural sketch of the same area. (c) Zoning across one of the Ca-rich parts of garnet2 (line in Fig. 5a). (d) Profile of similar length from garnet1 between matrix and inclusion feldspar ('B' of Fig. 3a) show lower peak Ca but higher Mg/(Mg+Fe) than garnet2.

is a regular feature of granulites from this region). The growth of a corona-like garnet enclosing spinel in many of these domains must, however, be evidence for the re-crossing of at least reaction (1) with an additional possible reaction being:

almandine-grossular(in garnet) + rutile =
  anorthite (in feldspar) + ilmenite + quartz (4)

Determination of $P-T$ conditions for the initial garnet consumption and the second garnet growth is not straightforward, as both garnet types show strong compositional variation. For reactions (1, 2 and 3) taking garnet1 rim and any plagioclase composition between An_{90} (a typical value for feldspar with spinel forming after kyanite) and An_{40} (the value measured in an inclusion in garnet2) yields pressures below 4 kbar for any

temperature below 1000°C (method of Berman (1991), with the activity models for garnet and feldspar from Berman (1990) and Fuhrmann and Lindsley (1988), respectively). Pairing the high-Ca garnet1 interior with secondary plagioclase (as opposed to primary ternary feldspar) yields values between 8.5 kbar (at 600°C) and 12 kbar (at 1000°C) for the same reactions. In all cases the reaction curves are in the stability field of sillimanite (thus consistent with the growth of secondary sillimanite in many felsic granulites). Interestingly, garnet growth by reaction (4) yields pressures above 7 kbar, at any temperature above 750°C and for any feldspar composition, when calculations are made with the first-formed Ca-rich part of garnet2. These results could be interpreted to reflect an initial decompression

into the sillimanite field at high temperature (kyanite breakdown) followed by near isobaric cooling along with secondary garnet growth in the kyanite breakdown domain. The shape of this path was similar to that proposed by Carswell and O'Brien (1993) and Petrakakis and Jawecki (1995) (albeit at different temperature conditions) for comparable granulites in Austria.

Discussion

The interpretation of garnet zoning profiles in terms of temperature-time paths has become popular in recent years as consistent experimentally-determined diffusion coefficients have become available and accurate measurement of zoning profiles by electron microprobe has become standard practice (e.g. Lasaga *et al.*, 1977; Lasaga, 1983; Loomis *et al.*, 1985; Jiang and Lasaga, 1990; Chakraborty and Ganguly, 1990, 1992; O'Brien and Vrána, 1995, 1997; O'Brien, 1997; Brenker and Brey, 1997; Duchêne *et al.*, 1998). A common assumption in these studies is that cubic garnet can be modelled effectively as a sphere with diffusion rates independent of crystallographic orientation. Then, by assuming a faster rate of transport of material to the garnet surface than within the garnet itself, grain-boundary transport rates can be ignored and the penetration depth of the measured compositional profile from the rim to interior of the garnet, fitted to a temperature-time model based on its diffusivities alone. For such models to be valid it is necessary that compositional profiles in garnet are the same regardless of direction. The asymmetric, one-sided profiles shown in Fig. 4c and f are inconsistent with the fast grain-boundary transport assumption. In fact, the profiles in Fig. 4c and f and the large difference in garnet rim X_{Mg} for opposite sides of the same grain can only be explained if material transport from the biotite-bearing zone along the garnet grain-boundary to the side away from the biotite zone is as slow as the volume diffusion within the garnet itself. As pointed out in the review by Joesten (1990), the actual diffusion process along the grain-boundary region will be faster than volume diffusion, but the total mass transfer is small due to its low cross-sectional area and so concentration contours effectively migrate as for volume diffusion. The possible location of biotite in the third dimension is difficult to control in a thin-section but the Mg compositional map in Fig. 4a, when compared

with the textural sketches (Figs. 2 and 4b) and line profiles (e.g. Fig. 4e vs. Fig. 4f), would most certainly appear to support a direct relationship between distance from biotite and modification of X_{Mg} in garnet. The result obtained from this study is very similar to the spatial variation in garnet-biotite Fe-Mg reported by Florence and Spear (1995), albeit in a lower temperature scenario, also attributed to relatively slow (within one order of magnitude of the garnet volume diffusion rate) grain-boundary transport. Extrapolating this result from major- element disequilibrium to trace-element or isotopic disequilibrium, it must be presumed that the effective lack of communication between mineral phases will lead to the preservation of a non-equilibrium state for these components also. For this reason, closure temperature models linking age and temperature on a presumed temperature-time path (e.g. Dodson, 1973, 1986; Ehlers and Powell, 1994; Jenkin *et al.*, 1994) using garnet as a geochronometer would attribute recorded ages as minimum ages where in fact the garnets could still be preserving distributions at, or very close to, those of the peak temperature stage.

Although the asymmetric trend in X_{Mg} in some garnets can be clearly attributed to communication with biotite, this is only part of the garnet zonation story. All the profiles show a decrease in Ca at their margins that is tied to a slight increase in X_{Mg}. The increase in X_{Mg} is seen both at margins with low X_{Mg} (i.e. close to biotite) and with high X_{Mg} (away from biotite, next to inclusions). Significantly, the Ca profile in garnet1 is essentially identical at its rim and at contacts with inclusion feldspars (Fig. 3c: compare also Fig. 5d). How can this be explained? Assuming breakdown of garnet to form anorthite by reaction (1), driven by a requirement for a more calcic feldspar and a less calcic garnet (i.e. a reaction at lower pressure), would explain the Ca depletion in garnet. At the same time, however, one would expect to see an increase in Fe and Mg but at a constant Mg/(Fe+Mg) and not, as seen here, with a rising X_{Mg}. If reaction (1) took place in conjunction with a reaction controlling Fe-Mg exchange it would have to be explained why X_{Mg} was different in different places although X_{Ca} was essentially the same at all rims. In addition, the inclusions are effectively shielded from any possible externally-controlled Fe-Mg exchange and yet they also show the same rise in X_{Mg}. A possibility that gradients in thermodynamic

activities in garnet would be reduced by increasing X_{Mg} at falling Ca was also tested (with the model of Berman, 1990) but for the dominant component, almandine, the measured compositional pattern towards the rim was shifted perpendicular to the non-ideal activity trend (i.e. with a stronger gradient) rather than at a low angle to it as would be the case for Ca decrease at constant X_{Mg}. Regardless of the explanation for this aspect, the important point is that this trend of rising X_{Mg} at garnet rims is also found on the biotite-bearing sides of one-sided profiles (Fig. 4c,f) and so most likely represents a processs post-dating biotite growth. The similarity of profiles to rims and inclusions (e.g. Fig. 3,c) suggests the lack of any enhanced diffusion with the aid of a grain-boundary fluid phase — garnet is subordinate to feldspar in the rock and so potentially could deliver all its excess Ca to Feldspar domains — and so once again points to a diffusion process under essentially dry conditions.

It is clear from textural criteria that biotite replaces garnet, and as no other hydrous phases are present, this reaction stage requires the influx of a fluid phase. However, if any free fluid had remained in the rock, it would have provided an interconnecting grain-boundary film that would have driven material transport faster between, than within, garnet grains. This was obviously not the case in this sample. Therefore, and this is a critical point in the discussion, this fluid-present stage must represent only a very short time period within a history dominated by fluid-absent conditions. This is essentially the scenario envisaged by Yardley and Valley (1997), i.e. the absence of a free, connected fluid phase in deep crustal rocks over any significant time period.

In conclusion it can be stated that, despite very high-temperature conditions during exhumation, rocks remaining essentially dry for the majority of their history can preserve compositional information that would otherwise be expected to be modified or smoothed by diffusion. Simply assuming that compositions must have been modified could lead to significant confusion in age determination by closure temperature models, in cooling rate estimation from the penetration depth of zoning at grain rims, and in selection of mineral compositions for geothermobarometry.

References

Aftalion, M., Bowes, D.R. and Vrána, S. (1989) Early Carboniferous U-Pb zircon age for garnetiferous perpotassic granulites, Blanský les massif, Czechoslovakia. *Neues Jahrb. Mineral., Mh.*, 145–52.

Becker, H. (1997) Sm-Nd garnet ages and cooling history of high-temperature garnet peridotite massifs and high-pressure granulites from lower Austria. *Contrib. Mineral. Petrol.*, **127**, 224–36.

Becker, H. and Altherr, R. (1991) Al-rich sapphirine in a high-P charnockite: reaction textures and P-T-evolution. *Terra abstracts*, **3**, 437.

Bégin, N.J. and Pattison, D.R.M. (1994) Metamorphic evolution of granulites in the Minto Block, northern Québec: extraction of peak *P-T* conditions taking account of late Fe-Mg exchange. *J. Metam. Geol.*, **12**, 411–28.

Behr, H.-J. (1978). Subfluenz-Prozesse im Grundgebirgs-Stockwerk Mitteleuropas. *Z. dt. geol. Ges.*, **129**, 283–318.

Berman, R.G. (1990) Mixing properties of Ca-Mg-Fe-Mn garnets. *Amer. Mineral.*, **75**, 328–44.

Berman, R.G. (1991) Thermobarometry using multi-equilibrium calculations: a new technique with petrological applications. *Canad. Mineral.*, **29**, 833–55.

Brenker, F.E. and Brey, G.P. (1997) Reconstruction of the exhumation path of the Alpe Arami garnet-peridotite body from depths exceeding 160 km. *J. Metam. Geol.*, **15**, 581–92.

Burton, K.W. and O'Nions, R.K. (1991) High resolution garnet chronometry and the rates of metamorphic processes. *Earth Planet. Sci. Lett.*, **107**, 649–71.

Carswell, D.A. and O'Brien, P.J. (1993) Thermobarometry and geotectonic significance of high pressure granulites: examples from the Moldanubian Zone of the Bohemian Massif in Lower Austria. *J. Petrol.*, **34**, 427–59.

Carswell, D.A., Möller, C. and O'Brien, P.J. (1989) Origin of sapphirine symplectites in metabasites from Mitterbachgraben, Dunkelsteinerwald granulite complex, Lower Austria. *Eur. J. Mineral.*, **1**, 455–66.

Chakraborty, S. and Ganguly, J. (1990) Compositional zoning and cation diffusion in aluminosilicate garnets. In *Diffusion, atomic ordering and mass transfer*. (J. Ganguly, ed.), Advances in Physical

Geochemistry Vol 8. Springer, New York, pp. 120–75.

Chakraborty, S. and Ganguly, J. (1992) Cation diffusion in aluminosilicate garnets: experimental determination in spessartine-almandine diffusion couples, evaluation of effective binary diffusion coefficients, and applications. *Contrib. Mineral. Petrol.*, **111**, 74–86.

Dodson, M.H. (1973) Closure temperature in cooling geochronological and petrological systems. *Contrib. Mineral. Petrol.*, **40**, 259–74.

Dodson, M.H. (1986) Closure profiles in cooling systems. *Materials Sci. Forum*, **7**, 145–54.

Duchêne, S., Albarède, F. and Lardeaux, J.-M. (1998) Mineral zoning and exhumation history in the Münchberg eclogites (Bohemia). *Amer. J. Sci.*, **298**, 30–59.

Ehlers, K. and Powell, R. (1994) An empirical modification of Dodson's equation for closure temperature in binary systems. *Geochim. Cosmochim. Acta*, **58**, 241–8.

Ferry, J.M. and Spear, F.S. (1978) Experimental calibration of the partitioning of Fe and Mg between biotite and garnet. *Contrib. Mineral. Petrol.*, **66**, 113–7.

Fiala, J. (1995) General characteristics of the Moldanubian Zone. In *Pre-Permian geology of Central and Eastern Europe*, (R.D. Dallmeyer, W. Franke and K. Weber, eds.), Springer, pp.417–8.

Fiala, J., Matějovská, O. and Vaňková, V.B. (1987). Moldanubian granulites: source material and petrogenetic considerations. *Neues Jahrb. Mineral. Abh.*, **157**, 133–65.

Florence, F.P. and Spear, F.S. (1995) Intergranular diffusion kinetics of Fe and Mg during retrograde metamorphism of a pelitic gneiss from the Adirondack Mountains. *Earth Planet. Sci. Lett.*, **134**, 329–40.

Fuchs, G. (1971) Zur Tektonik des östlichen Waldviertels (N. Ö.). *Verh. Geol. B-A., Wien*, **3**, 424–40.

Fuchs, G. (1991) Das Bild der Böhmischen Masse im Umbruch. *Jahrb. Geol. B-A., Wien* **134**, 701–10.

Fuchs, G. (1995) The Austrian part of the Moldanubicum. In *Pre-Permian geology of Central and Eastern Europe,* (R.D. Dallmeyer, W. Franke and K. Weber, eds.), Springer, pp. 422–6.

Fuhrmann, M.L. and Lindsley, D.H. (1988) Ternary-feldspar modelling and thermometry. *Amer. Mineral.*, **73**, 201–15.

Jenkin, G.R.T., Farrow, C.M., Fallick, A.E. and Higgins, D. (1994) Oxygen isotope exchange and closure temperatures in cooling rocks. *J. Metam. Geol.*, **12**, 221–36.

Jiang, J. and Lasaga, A.C. (1990) The effect of post-growth thermal events on growth-zoned garnet:

implications for metamorphic P-T history calculations. *Contrib. Mineral. Petrol.*, **105**, 454–9.

Joesten, R. (1990) Grain boundary diffusion kinetics in silicate and oxide minerals. In *Diffusion, atomic ordering and mass transfer,* (J. Ganguly, ed.), Advances in Physical Geochemistry Vol **8**, Springer, New York, pp. 345–95.

Kotková, J., Kröner, A., Todt, W. and Fiala, J. (1996) Zircon dating of North Bohemian granulites, Czech Republic: further evidence for the Lower Carboniferous high-pressure event in the Bohemian Massif. *Geol. Rundsch.,* **85**, 154–61.

Kotková, J. and Harley, S.L. (1997) Mineral controls on the trace element and REE geochemistry of high-pressure leucogranulites from the Bohemian Massif. *J. Czech. Geol. Soc.,* **42**, 40.

Koziol, A.M. and Newton, R.C. (1989) Grossular activity-composition relationships in ternary garnets determined by reversed displaced-equilibrium experiments. *Contrib. Mineral. Petrol.,* **103**, 423–33.

Kröner, A., Jaekel, P., Reischmann, T. and Kroner, U. (1998) Further evidence for an early Carboniferous (~340 Ma) age of high-grade metamorphism in the Saxonian granulite complex. *Geol. Rundsch.,* **86**, 751–66.

Kröner, A. and Willner, A.P. (1995) Magmatische und metamorphe Zirkonalter für Quarz-Feldspat-Gesteine der Gneis-Eklogit-Einheit des Erzgebirges. *Terra Nostra,* **95/8**, 112.

Kryza, R., Pin, C. and Vielzeuf, D. (1996) High pressure granulites from the Sudetes (SW Poland) evidence of crustal subduction and collisional thickening in the variscan Belt. *J. Metam. Geol.,* **14**, 531–46.

Lasaga, A.C. (1983) Geospeedometry: an extension of geothermobarometry. In *Kinetics and equilibrium in mineral reactions,* (S.K. Saxena, ed.), Advances in Physical Geochemistry Vol 3, Springer, pp. 81–114.

Lasaga, A.C., Richardson, S.M. and Holland, H.D. (1977) The mathematics of cation diffusion and exchange between silicate minerals during retrograde metamorphism. In *Energetics of Geodynamic Process,* (S.K. Saxena and S.D. Bhattacharji, eds.), Springer, New York, pp. 353–88.

Loomis, T.P., Ganguly, J. and Elphick, S.C. (1985) Experimental determination of cation diffusivities in aluminosilicate garnets II. Multi-component simulation and tracer diffusion coefficients. *Contrib. Mineral. Petrol.,* **90**, 45–51.

Medaris, Jr., L.G. and Carswell, D.A. (1990) Petrogenesis of Mg-Cr garnet peridotites in European Metamorphic belts. In *Eclogite Facies Rocks,* (D.A. Carswell, ed.), Blackie, Glasgow, pp. 260–90.

Medaris, Jr., L.G., Beard, B.L., Johnson, C.M., Valley, J.W., Spicuzza, M.J., Jelínek, E. and Mísaø, Z. (1995) Garnet pyroxenite and eclogite in the

Bohemian Massif: geochemical evidence for Variscan recycling of subducted lithosphere. *Geol. Rundsch.*, **84**, 489−505.

Neumann, W. (1984) Zur erdgeschichtlichen Entwicklung des sächsischen Granulitmassivs. *Z. angew. Geol*, **30**, 183−90.

O'Brien, P.J. (1997) Granulite facies overprints of eclogites: short-lived events deduced from diffusion modeling. In *Precambrian Geology and Metamorphic Petrology*, (X. Qian, Z. You and H.C. Halls, eds.), Proceedings of the 30th International Geological Congress, vol 17, VSP, Utrecht, Netherlands, pp. 157−71.

O'Brien, P.J. and Vrána, S. (1995) Eclogites with a short-lived granulite facies overprint in the Moldanubian Zone, Czech Republic: petrology, geochemistry and diffusion modelling of garnet zoning. *Geol. Rundsch.*, **84**, 473−88.

O'Brien, P.J. and Vrána, S. (1997) The eclogites in the Monotonous Series of the Moldanubian Zone and the theory of thermal pulses: a reply. *Geol. Rundsch.*, **86**, 716−9.

O'Brien, P.J., Kröner, A., Jaekel, P., Hegner, E., Żelaźniewicz, A. and Kryza. R. (1997). Petrological and isotopic studies on Palaeozoic high pressure granulites with a medium pressure overprint, Góry Sowie (Owl) Mts., Polish Sudetes. *J. Petrol.*, **38**, 433−56.

Owen, J.V. and Dostal, J. (1996) Contrasting corona structures in mafic granulite from the Blansky les complex, Bohemian Massif, Czech Republic. *Canad. Mineral.*, **34**, 959−66.

Petrakakis, K. and Jawecki, C. (1995) High-grade metamorphism and retrogression of Moldanubian granulites, Austria. *Eur. J. Mineral.* **7**, 1183−203.

Pin, C. and Vielzeuf, D. (1983) Granulites and related rocks in Variscan median Europe: a dualistic interpretation. *Tectonophysics,* **93**, 47−74.

Quadt, A. von (1993) The Saxonian Granulite Massif: new aspects from geochronological studies. *Geol. Rundsch.,* **82**, 516−30.

Schenk, V. and Todt, W. (1983) U-Pb Datierungen an Zirkon und Monazit der Granulite im Moldanubikum Niederösterreichs (Waldviertel). *Fortschr. Mineral.,* **61**, 190−1.

van Breemen, O., Aftalion, M., Bowes, D.R., Dudek, A., Mísař, Z., Povondra, P. and Vrána, S. (1982) Geochronological studies of the Bohemian Massif, Czechoslovakia, and their significance in the evolution of Central Europe. *Trans. R. Soc. Edinburgh: Earth Sci.,* **73**, 89−108.

Vrána, S. (1989) Perpotassic granulites from southern Bohemia. A new rock-type derived from partial melting of crustal rocks under upper mantle conditions. *Contrib. Mineral. Petrol.,* **103**, 510−22.

Vrána, S. and Jakeš, P. (1982) Orthopyroxene and two-pyroxene granulites from a segment of charnockitic crust in southern Bohemia. *Bull. Geol. Surv. Prague,* **57**, 129−43.

Wendt, J.I., Kröner, A., Fiala, J. and Todt, W. (1994) U-Pb zircon and Sm-Nd dating of Moldanubian HP/HT granulites from South Bohemia, Czech Republic. *J. Geol. Soc. Lond.,* **151**, 83−90.

Willner, A.P., Rötzler, K. and Maresch, W. (1997) Pressure-temperature and fluid evolution of quartzo-feldspathic metamorphic rocks with a relic high-pressure, granulite-facies history from the Central Erzgebirge (Saxony, Germany). *J. Petrol.,* **38**, 307−36.

Yardley, B.W.D. and Valley, J.W. (1997) The petrologic case for a dry lower crust. *J. Geophys. Res.,* **102**, 12173−85.